# First direct observation of the quantum mechanical behaviour of a truly macroscopic object

Helvetica Physica Acta,
Vol. 56 (1983) 789-795

0018-0238/83/010789-07$1.50+0.20/0


# FIRST DIRECT OBSERVATION OF THE QUANTUM MECHANICAL BEHAVIOUR OF A TRULY MACROSCOPIC OBJECT

R.J. Prance+, J.E. Mutton+, H. Prance+, T.D. Clark+, A. Widom* and G. Megaloudis*, (+Physics Dept., University of Sussex, Brighton, Sussex, England and *Physics Dept., Northeastern University, Boston, Mass., U.S.A.)

It is well known that the current-carrying state in a thick superconducting ring can be characterised by the integer number (n for $n \cdot 2\pi$) or "winding number" of the electron pair condensate phase, where $n = 0, \pm 1, \pm 2, \ldots$ If the ring is subjected to an external applied flux $\Phi_x$, the magnetic field energy storage in the ring is given by

$$W_n(\Phi_x) = (n\Phi_0 - \Phi_x)^2/2\Lambda \qquad (1)$$

where $\Phi_0 = h/2e$, $\Lambda$ is the geometric inductance of the ring and $n\Phi_0$ is the quantised flux trapped in the ring at $\Phi_x = 0$.

The well known experimental technique adopted to facilitate transitions between winding-number states is to include a "Josephson" weak link in the ring[1]. Quantum-mechanically, the effect of this weak link is to connect states of different winding number (here, referred to as the principal quantum number) by the coherent transfer of magnetic flux bundles ($\Phi_0$) across the weak link. Quantum-electrodynamically, this transfer can be considered to constitute the second or "conjugate" Josephson effect, by analogy with the coherent transfer of superconducting pairs through a weak link. We note that in this quantum electrodynamic view[2] the flux ($\Phi$) in the ring inductor ($\Lambda$) and the charge (Q) included on the weak-link capacitor ( C) become associated with non-commuting operators $Q \to i\hbar\partial/\partial\Phi$ or $\Phi \to -i\hbar\partial/\partial Q$ such that $[\Phi, Q] = -i\hbar$. In the simplest theoretical model of a weak-link ring we can restrict transitions to nearest-neighbour winding-number states (i.e. $n \to n \pm 1$) with a transition matrix element $\hbar\Omega/2$, where $\Omega$ is the frequency for the coherent transfer of flux bundles across the weak link. If $D_n$ is the amplitude for the ring to have a winding number n then we can construct a Schrödinger equation to describe this infinite set of nearest-neighbour transitions in terms of the above matrix element and equation (1). This equation, which is of the form

$$W_n(\Phi_x)D_n - (\hbar\Omega/2)(D_{n+1} + D_{n-1}) = ED_n \qquad (2)$$

allows us, for the case of "weak coupling" ($\hbar\Omega$ small), to calculate the lowest-lying energy level of the weak-link ring accurately. Here, each winding-number transition ($\pm 1$) corresponds to a quantised flux change ($\pm\Phi_0$) in the ring.

Equation (2) takes on a more familiar form when we make the transformation from a winding number (n) to an angular ($\theta$) representation[3], i.e. in terms of the angular rotation $\theta$ of the electron pairs in the ring as a whole. The macroscopic wave function describing the complete electron pair condensate as a single quantum object is $\psi(\theta) = \sum_n D_n e^{in\theta}$ which obeys the transformed equation (2)

$$(1/2\Lambda)[-i\Phi_0(\partial/\partial\theta)-\Phi_x]^2\psi(\theta) - \hbar\Omega \cos\theta\ \psi(\theta) = E\psi(\theta) \qquad (3)$$

where the energy-level solutions of this equation are periodic in $\Phi_x$, i.e. form "energy bands" such that $E_\kappa(\Phi_x + \Phi_0) = E_\kappa(\Phi_x)$. In terms of these solutions the screening supercurrent and magnetic moment polarizability of the weak-link ring are given by $I_s = -(dE_\kappa/d\Phi_x)$ and $\chi = \Lambda(d^2E_\kappa/d\Phi_x^2)$, respectively. We note that the energy bands ($E_\kappa$ versus $\Phi_x$) are constructed from a coherent amplitude superposition of winding-number states of the ring in which the "good quantum number" is now $\kappa$ not n.

Fine-Structure Quantum Numbers

In the conventional theory[4] of the Josephson weak link there exists a "plasma frequency" $\omega_0$ for the link given by $\omega_0^2 = (1/\Lambda_{eff}\ C)$ where $\Lambda_{eff}$ and C are, respectively, the effective inductance and the capacitance of the weak link. For the weak link contained within a ring, $\omega_0$ takes the form of a coupled plasma oscillation with $(1/\Lambda_{eff}) = (1/\Lambda) + (4e^2\nu/h)$, where $h/4e^2\nu$ is the "kinetic" inductance of the weak link and $\nu$ is the Josephson pair transfer frequency through the link. To include these excitations (energy $m\hbar\omega_0$, m = 0,1,2, 3,...,) in the macroscopic Schrödinger equation we can simply write the amplitude (above) as $\psi(\theta,m)$ where m is the number of photon excitations. In the $\theta$-representation the Schrödinger equation (3) now has the form

$$(1/2\Lambda)[-i\Phi_0(\partial/\partial\theta)-\Phi_x]^2\psi(\theta,m) + m\hbar\omega_0\psi(\theta,m) -$$
$$\hbar \sum_{m'} \Omega_{mm'} \cos\theta\,\psi(\theta,m') = E\psi(\theta,m) \qquad (4)$$

where the matrix element $\Omega_{mm'}$ for m' photons to go into m photons during a $n \to n \pm 1$ transition is given in terms of combinational factors (with r going from zero to the minimum of m and m'), and a factor $\lambda$ acting as a coupling parameter linking winding number and photon transitions together, by

$$\Omega_{mm'} = \Omega \sum_r \sqrt{m!m'!}\,[r!(m-r)!(m'-r)!]^{-1}\,\lambda^{(m+m'-r)}. \qquad (5)$$

Again, the Schrödinger equation (4) yields energy bands ($E_\kappa$ versus $\Phi_x$), with good quantum number $\kappa$, but now these bands are created from an amplitude superposition of different winding number and photon excitation states.

## The Weak-Link Ring Band-Structure Measurement Technique

In principle the technique we use to monitor the energy-band structure of a weak link ring as a function of $\Phi_X$ is extremely simple although in practice it has required us to develop a state of the art UHF receiver with an effective system noise temperature ($T_N$) ≃ few K. Imagine, first, an inductor (L), narrow-banded by a capacitor connected in parallel, at a temperature T. If the centre frequency of this tuned ("tank") circuit is $\omega_R$, such that $\hbar\omega_R \ll k_BT$, then the inductor L will act as a "classical object" and the flux noise in this inductor, integrated over the band pass of the tank circuit, will be just $\langle\Delta\Phi^2\rangle = k_BTL$. If this tank circuit inductor is coupled through a mutual inductance M to a weak-link ring of magnetic-moment polarizability $\chi = \Lambda(d^2E_K/d\Phi_X^2)$, we have shown elsewhere that the flux noise in the inductor is now given by[5]

$$\langle\Delta\Phi^2\rangle = k_BTL\,[1 + K^2\Lambda.\,(d^2E_K/d\Phi_X^2)] \qquad (6)$$

where, as usual, $K^2 = M^2/L\Lambda$ and here the external flux $\Phi_X$ is controlled by a slowly varying current $I_X$ flowing through a bias coil coupled to the weak-link ring.

The very-low-noise-temperature receiver system we use to measure these flux fluctuations is shown in block form in figure 1. We have chosen 430 MHz as the centre frequency of this receiver (bandwidth ≃ 35 MHz) partly for historical reasons[1] but also because of the ready availability of very low-noise GaAs devices in this frequency range. The receiver is power-matched capacitively to the LC "tank" circuit under loaded conditions, i.e. with the tank circuit coil coupled to the weak-link ring. The quality (Q) factor for the ring-tank circuit combination is approximately 40. The approximate noise temperatures, and operating temperatures, for each amplification stage of the receiver are given in figure 1. The particular features to note about this system, apart from its amplification stages, are (1) an extremely stable local oscillator [few parts in $10^{10}$ frequency stability] (ii) a properly broad-band matched and terminated input to the IF amplifier (iii) very broad-band noise isolation between

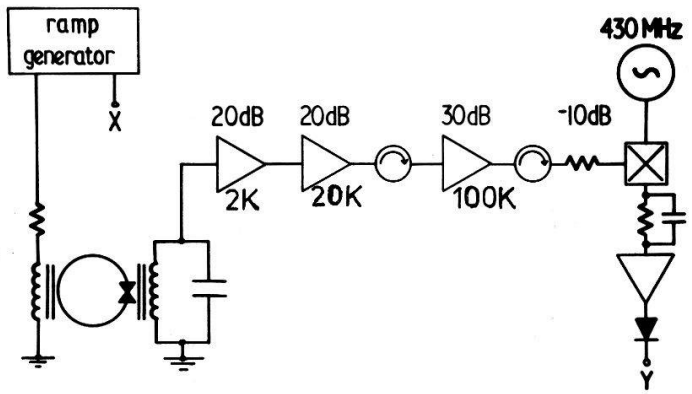


Figure 1

the room temperature electronics system and the 430 MHz resonator circuit and (iv) massive electromagnetic shielding for the receiver and the low-temperature circuitry. We note that for the double-derivative noise spectroscopy technique to work, as expressed in equation (6), the effective "environmental" noise temperature $T_{NAR}$ created by the receiver (i.e. measurement) system at the weak-link ring must be less than the ambient (bath) temperature T of the ring, i.e. for T = 4.2K, $T_{NAR} \lesssim$ few K. This can be achieved provided (i) the system is operated narrow-band and (ii) the first and second-stage amplifiers are cryogenically cooled.

The experimental technique used to observe the magnetic moment polarizability $\chi$ of the ring is very simple. We adjust all the UHF (+ output) amplifier stages for minimum noise temperature and plot the mean square flux noise $\langle \Delta\Phi^2 \rangle$ generated in the tank-circuit coil, integrated over the tank-circuit bandpass, as a function of a slowly varying external flux $\Phi_{XDC}$. The output of the receiver is displayed on a standard x versus t plotter with a bandwidth from DC to a few Hz. Typically noise plots, extending over 10 to 20 $\Phi_0$ of external bias flux (both positive and negative), are recorded over time periods of up to five minutes.

## The Weak-Link Ring

It is clear from equations (3) and (4) that macroscopic quantum-mechanical effects will be most readily observable if $\hbar\Omega$ and $\hbar\omega_0$ are large, i.e. if the cross-section of the weak link in the ring is made as small as possible ( $\sim$ a few superconducting penetration depths $\lambda$ across). At the present state of superconducting device technology these requirements can still be best achieved by working with rings containing point-contact constriction weak links. Mechanical and thermal stability is achieved in practice by making use of the so-called "Zimmerman" two-hole structure [1], as depicted in figure 2.

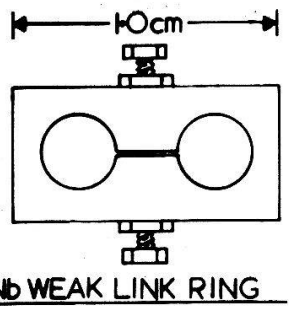

Figure 2

In our devices [6] the block, screw and mechanical lock nuts are machined from niobium and the mechanically stabilised point contact is oxidised before the final adjustment is made. Typically, with these point contacts adjusted to have maximum sustainable supercurrents in the $\mu$A range ($\nu \simeq 10^{13}$ Hz) the effective capacitance (C) and cross section ($d^2$), as inferred from other experiments [3], appear to be $\leq 10^{-15}$ F and $\leq$ 1000Å square, respectively.

Magnetic Polarizabilities

In figure 3a we show an experimental plot of $\langle\Delta\Phi^2\rangle$ versus $\Phi_{XDC}$ with the UHF receiver set for minimum noise temperature. Here, the maximum sustainable supercurrent in the weak-link ring used in this experiment was in the μA range and T = 4.2K. We can see that the output of the receiver as a function of $\Phi_{XDC}$ is a series of noise spikes, separated by precisely (to better than 1% accuracy) $\Phi_0$ intervals. The position of these spikes on the $\Phi_{XDC}$ axis is the same when the input bias coil current ($\Phi_{XDC}$) is reversed to sweep the flux between ± $20\Phi_0$, i.e. there is no observable hysteresis.

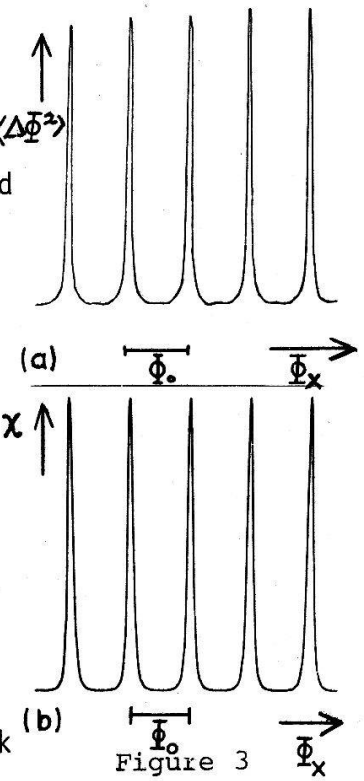

Figure 3

What we are seeing in figure 3a is the external flux-dependent magnet-moment polarizability of the weak-link ring in the lowest ($\kappa$=1) band solution of the Schrödinger equation (4). In figure 3b we show $\chi(\kappa=1)$ versus $\Phi_{XDC}$, calculated from the lowest band (m=0) solution of equation (4) with $\Omega$ taken, for best fit, from the experimental linewidth of the spikes in figure 3a, i.e. with $\hbar\Omega$ = 0.05 $\Phi_0^2/\Lambda$, where $\Phi_0^2/\Lambda$ can be considered to be the natural scaling energy for the weak link ring.

We have been able to make use of a very convenient experimental technique to kick the weak-link ring from one energy band to another, at least for the lowest bands. It is well known that the excess noise temperature of a high performance GaAs FET amplifier is a function of the gate voltage ($V_G$) applied. In most circumstances it is the "in-band" (e.g. for us 430±15 MHz) noise of the amplifier which is of interest. However, it should be appreciated that these devices produce noise up to extremely high frequencies ($\gtrsim$ 50 GHz). When $V_G$ is adjusted the level of all these noise components is changed, including those at many tens of GHz. It is these extremely high-frequency-noise photons that we have utilised to kick the weak-link ring between the various low-lying allowed bands. Our technique is to adjust $V_G$ on the second stage GaAs FET amplifier (at 77K) to change the in-band noise temperature ($T_{NA2}$) by ± few K. Now, with an estimated 30 dB of in-band reverse isolation between this amplifier and the weak link ring, a 10K adjustment in $T_{NA2}$ results in a 0.1K change in $T_{NAR}$. This is negligible in terms of the

large flux-transfer frequency ($\Omega$) implied by figure 3a. However, even though the in-band reverse isolation is good, our receiver system is virtually transparent to injected noise above 5 GHz. It appears, therefore, that when we change $V_G$ on the second (or other) stage amplifier we inject a burst of extremely high-frequency-noise photons into the low-temperature system. This acts to kick the weak-link ring from band to band. We emphasise that we are dealing with a single quantum object so in no sense is there a Boltzmann distribution for this "particle" in the various available bands on the timescale of a single sweep in $\langle\Delta\Phi^2\rangle$ versus $\Phi_{XDC}$.

In figure 4a we show experimental plots of $\langle\Delta\Phi^2\rangle$ versus $\Phi_{XDC}$ at T = 4.2K for the weak-link ring kicked into the second band in external flux space. We see that the original noise spikes of figure 3a have "split" in a characteristic manner. We can generate such a pattern from the second band (m=1) solution of equation (4). In figure 4b we show the $\chi(\kappa=2)$ versus $\Phi_{XDC}$ pattern calculated from this second band solution with, as before, $\hbar\Omega = 0.05\Phi_0^2/\Lambda$ and, for best fit, $\hbar\omega_0 = 0.078\Phi_0^2/\Lambda$. In both figures 4a and 4b the coupling parameter $\lambda$ is set at 0.5. We note that modest changes in $\lambda(0.5 \pm 0.2)$ have little effect on the theoretical polarizability patterns of figures 3b and 4b. These patterns have been suitably scaled on the vertical axis to match the experimental plots of figures 3a and 4a.

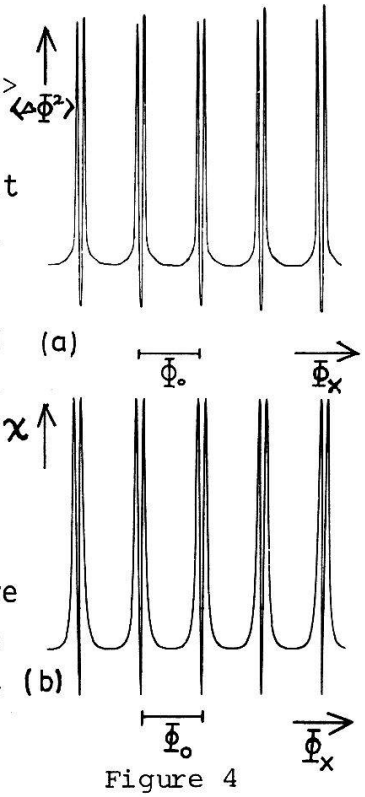

Figure 4

With definite values of the $\hbar\Omega$ and $\hbar\omega_0$ we can compute the lowest-lying bands ($E_K$ versus $\Phi_{XDC}$) for the above point-contact weak-link ring. The first three bands are shown in figure 5 with $\hbar\Omega = 0.05\ \Phi_0^2/\Lambda$, $\hbar\omega_0 = 0.078\Phi_0^2/\Lambda$ and $\lambda = 0.5$ The energy spacing between these bands at $\Phi_{XDC} = 0$ is $\hbar\omega_0$. We

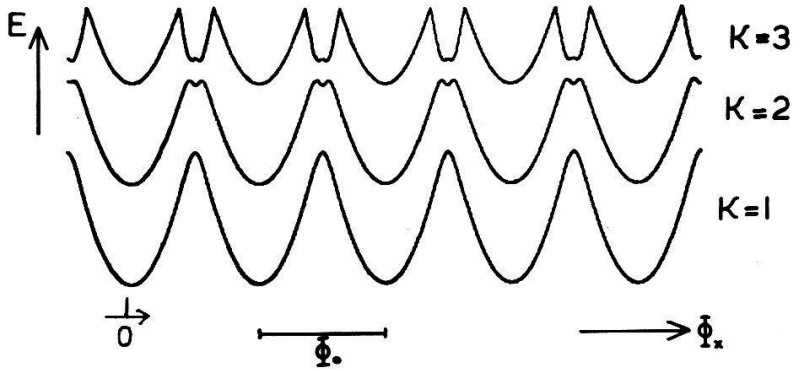

Figure 5

see that the third band-scheme solution has an elaborate structure which generates a very characteristic second-derivative polarizability pattern. This is shown in figure 6a and we see that the split noise spikes of figure 4a have split again. In figure 6b we show the experimental $\langle\Delta\Phi^2\rangle$ versus $\Phi_{XDC}$ plot for the weak-link ring kicked into the third (m=2) band. From the experimental plots (figures 3a, 4a and 6b) it is apparent that the weak-link ring can remain stably in a particular low-lying band for some considerable time - of the order of 1 to 2 minutes is typical for the UHF receiver system used in these measurements.

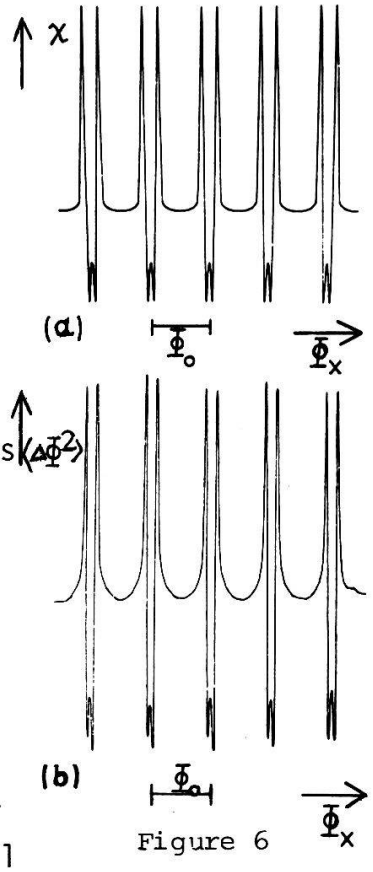

Figure 6

## Conclusions

From a theoretical viewpoint it is evident that superpositions of macroscopically different states exist as solutions to the Schrödinger equation. The experimental problem of observing such superpositions becomes that of reducing the random environmental noise sufficiently over the time required for the observation. It is apparent from figures 3,4 and 6 that we have now achieved this required degree of "electronic isolation". We note that for large-capacitance weak-link devices, such as the Josephson tunnel junction, $\hbar\omega_0$ will be very small. There is little doubt that at the present state of the electronic art such finely spaced levels would remain unresolved spectroscopically.

## Referencees

[1] J.E. Zimmerman and N.V. Frederick, Appl. Phys. Lett. 19, 16-19 (1971).

[2] A. Widom, G. Megaloudis, J. Sacco and T.D. Clark, Il Nuovo Cimento 61B, 112-122 (1981).

[3] C. Itzykon and J.B. Zuber, "Quantum Field Theory", 571 (McGraw-Hill 1980).

[4] See, for example, L. Solymar, "Superconductive Tunnelling and Applications" (Chapman and Hall, London 1972).

[5] A. Widom, G. Megaloudis, T.D. Clark and R.J. Prance, Il Nuovo Cimento 69A, 128-132 (1982).

[6] R.J. Prance, A.P. Long, T.D. Clark, A. Widom, J.E. Mutton, J. Sacco, M.W. Potts, G. Megaloudis and F. Goodall, Nature 289, 543-549 (1981).